

Numerical analysis of three-lobe journal bearing with CFD and FSI

Pankaj Khachane¹, Dinesh Dhande²

¹PG Student at Department of Mechanical Engineering, AISSMSCOE Pune, Maharashtra, India

²Assistant Professor at Department of Mechanical Engineering, AISSMSCOE Pune, Maharashtra, India

Abstract - The objective of this paper is to present a numerical analysis of the three-lobe journal bearing. The effects of this bearing are analyzed by using computational fluid dynamics (CFD) and Fluid Structure Interaction (FSI) technique. The pressure distribution and temperature distribution of the fluid film generated in the three-lobe hydrodynamic journal are obtained for different rotational speeds and eccentricity ratios. The study shows the appreciable changes in the performance characteristics due to bearing deformation.

Key Words: Three-lobe bearing, multi-lobe journal bearing, pressure distribution, temperature distribution.

1. INTRODUCTION

Recently, the output of internal combustion engines has been increased and their weight has been reduced. Due to this, bearings are forced to operate under stringent conditions and deformation of housings of connecting rod big-end bearings and main bearings have significant influence upon the bearing characteristics. Also, the increase in bearing loads and desire to reduce the dimensions and component masses obligates to make modification in the bearing.

Regarding journal bearings, the instability issue is introduced as a serious design parameter in rotating systems, especially for those of medium and high speed. Though the plain cylindrical journal bearing is generally used in the rotating machinery it does not satisfy the stability requirements of high speed machinery. In such specialized cases, plain circular bearings are replaced by non-circular journal bearings. Lobed bearing offers wide range of possibilities for providing the required stiffness and damping characteristics to the designed system and provides the required load capacity and stability. The geometric design parameters introduced with lobed journal bearings are the number of lobe, pads, pad orientations, clearances, preload factors, the centres of pad arc for each of the lobes forms a circle, referred to as a preload circle.

Relative motion in the bearing draws the oil into converging wedge, as relatively incompressible oil is forced out of the sides of the bearing; it modifies the clearance space which results in rise in pressure. The load imposed by the shaft is supported by the self-generated pressure around the bearing. Hence it is very much important to develop an analytical method to predict accurate performance of the bearing considering these realistic changes. R. Sinhasan et

al.[1] did the comparative study of some three-lobe bearing configuration which is based on the static and dynamic characteristics. S. C. Jain et al.[2] analyzed elasto-hydrodynamic effect on a cylindrical journal bearing with a flexible bearing shell to predict the performance characteristics of a hydrodynamic journal bearing. Villar M. M. et al.[3] carried out elastic analysis of journal bearing using commercial finite element software ANSYS and observed that the pressure distribution in the lubricant is significantly affected by the elasticity of the bearing. Banwait S. S.[4] analyzed the effect of journal misalignment on the thermohydrodynamic performance characteristics of non-circular two-lobe and three-lobe journal bearings. David V. Taylor[5] studied the static characteristics of highly preloaded three-lobe journal bearing. Maximum pressure occurred in the region of minimum film thickness is verified. The test rig used contains static loading system as well as dynamic loading system on a fixture. Measured pressure and film thickness profiles are shown as result. The relation between equilibrium attitude angle and eccentricity ratio has explained by Dr. Luis San Anders[6] which can be used to assume the attitude angle for three-lobe bearing calculation in this study. Zhi Li[7] has proposed Fourier analysis of three-lobe journal bearing. Here the coupling effect and inherent relevance is taken into account instead of considering each lobe separately. Pressure profiles obtained are similar for each lobe i.e. maximum pressure for each lobe is same. A. Chasalevris[8] explained analytical evaluation of the static and dynamic characteristics of three-lobe journal bearings with finite length using numerical methods for the solution of the Reynolds equation for the case of three-lobe bearings. D.Y. Dhande et al.[9] explained the multiphase flow phenomena of hydrodynamic journal bearing using fully three-dimensional CFD analysis considering the elastic deformations of the bearing with Fluid Structure Interactions (FSI) along with cavitation.

In this work, ANSYS 16.0 software is used to study the analytical results for three-lobe bearing model. Fluent tool is used for CFD analysis and System coupling tool is used for analyzing FSI. By the lobe profile the optimum operation of bearing can be achieved along with improved stability at higher speed and reduce the chances fatigue failure, thus improves performance of the bearing. Also, bearing absorbs several times more shock load, provides noise and wear free operation with more service life, cantered shaft position, good cooling effect and low friction losses are the advantageous over plane bearing.

2. GEOMETRY DESCRIPTION

The three-lobe journal bearing geometry used in the present work is shown in Fig. 1. The eccentricity 'e' is the distance between shaft and bearing centres. The external load 'W' is assumed as acting vertically along Y axis and is constant. The hydrodynamic pressure developed in the convergent region, separates the bearing from shaft with a fluid film and balances the external force acting on the shaft. Journal diameter 'D', its radius is R. The machined radial clearance of the lobes, common to all three lobes, is 'C' such that the radius of the curvature of the lobes is 'R+C'. The preload 'δ' is 'δ=r/c'. Thus, when δ=0, the bearing becomes cylindrical and when δ=1, the bearing touches all three lobes.

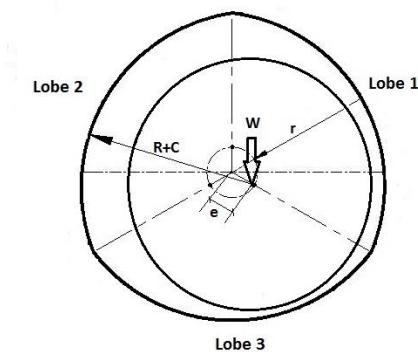


Fig -1: Three-lobe bearing geometry

3. METHODOLOGY

To analyze performance of the three-lobe journal bearing, computational fluid dynamics as well as two-way FSI is used. Structural deformations are analyzed using finite element structural module. These two modules are system coupled in order to transfer fluid forces developed due to fluid flow on bearing shell to compute elastic deformations in the shell. These deformations are again send back to modify the geometry in turn fluid domain through parametric modelling. Equilibrium position of the shaft is set. At equilibrium position, the fluid forces in the vertical direction (X-load) balance the shaft load and the fluid forces in the horizontal direction (Y-load) are zero. Initially, for given load and speed, the shaft rotation axis is fixed at a predefined position in terms of eccentricity and attitude angle in parametric form and the system is solved to get fluid forces in X and Y direction. The fluid forces are computed in computational fluid dynamics (CFD) domain and structural deformations are computed in structural domain. These two systems are system coupled to perform elasto-hydrodynamics. Fluid forces developed in CFD are transferred to the structural domain and vice versa in the system coupling.

4. ASSUMPTIONS AND BOUNDARY CONDITIONS

The Navier Stokes equations are solved using 3D double precision pressure based steady state analysis. As the

Reynolds number is very low, laminar and isothermal flow conditions are assumed. The solid domain, shaft and bearing are meshed using tetrahedral meshing. The lubricant supply hole is specified as 'pressure inlet' and the sides of the lubricant are specified as 'pressure outlet' with gauge pressure as zero. The inlet pressure is taken as 101.325 kPa. The bearing is modelled as 'stationary wall' and the shaft is modelled as 'moving wall' with absolute rotation speed. Initially the shaft axis position is defined by an arbitrary value of eccentricity and the attitude angle and these values are given as input to shaft rotation axis origin. To model the change in thickness of fluid domain, dynamic mesh technique in FLUENT is used. The mesh is then transferred to fluent for flow analysis. The smoothing mesh method is used number of iterations are 50. The fluid domain is meshed using hexahedral elements in CFD as shown in fig.2. The lubricant film is provided with 4 layers in radial direction and element size of 0.6 mm.

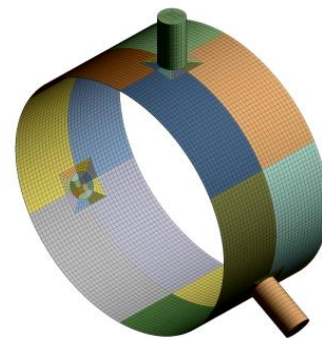


Fig -2: Geometry and mesh of fluid domain: oil film

4.1 Three-lobe Journal Bearing Parameters and Material Properties

Table -1: Material properties of the bearing:

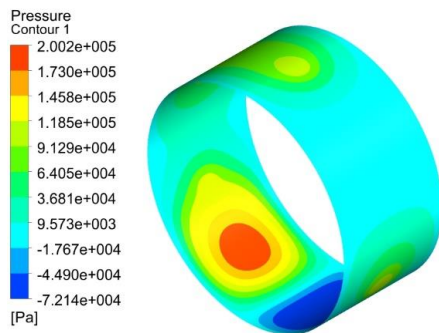
Parameter	Value
Journal diameter, D	50 mm
Clearance, C	50 μm
Preload circle, r	50 μm
Lobe radius, R+C	25.05 mm
Length of bearing, L	37.5 mm
Speed, N	1000,2000,3000,4000 RPM
Eccentricity ratio, ε	0.2, 0.4, 0.6, 0.8, 0.9
Lubricant Viscosity, μ	0.0143 Pa-sec
Lubricant Density, ρ	887 kg/m ³
oil vapour saturation pressure	29185 Pa
Material:	
Shaft: Structural Steel	Elastic Modulus = 200 GPa
	Density, ρ _s = 7850 kg/m ³
	Poisons ratio = 0.3
Bearing: Aluminium	Elastic Modulus = 68.9 GPa
	Density, ρ _A = 2700 kg-m ³
	Poison ratio = 0.33

5. RESULTS AND DISCUSSIONS

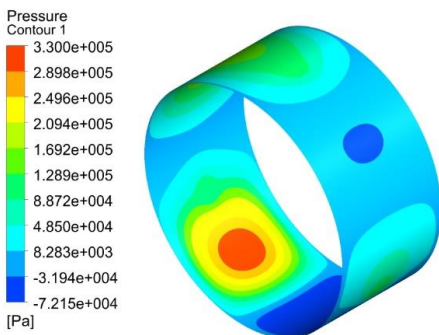
The three-lobe journal bearing were analyzed for eccentricity ratios viz. 0.2, 0.4, 0.6, 0.8 and 0.9 for various speeds 1000 RPM, 2000 RPM, 3000 RPM and 4000 RPM. The pressure and temperature plots were plotted for CFD considering with FSI technique.

The results of film pressure and temperature distribution for eccentricity ratio 0.4 and 1000, 2000, 3000, 4000 RPM are shown below:

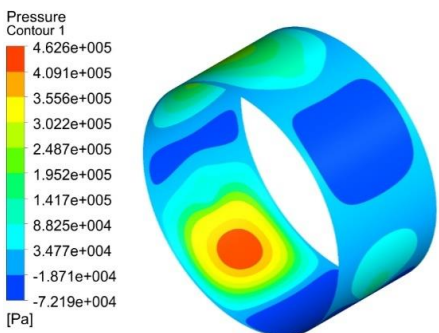
a) Pressure distribution contour for 1000RPM



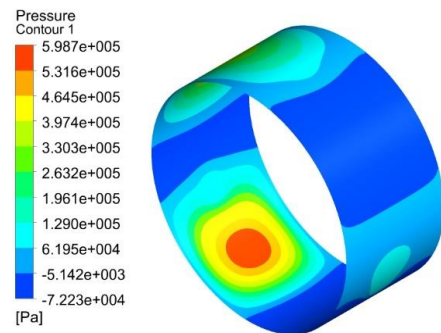
b) Pressure distribution contour for 2000RPM



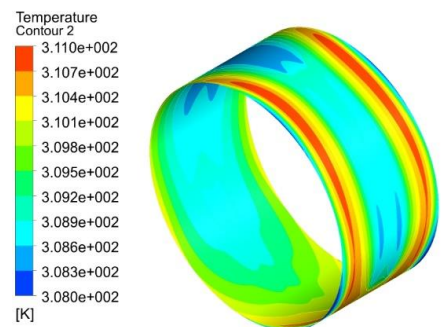
c) Pressure distribution contour for 3000RPM



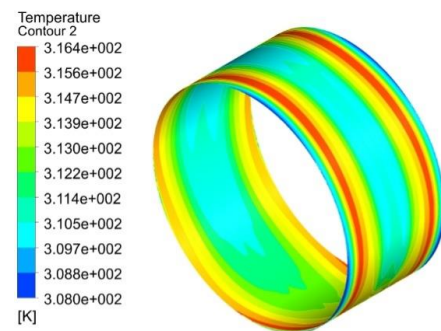
d) Pressure distribution contour for 4000RPM



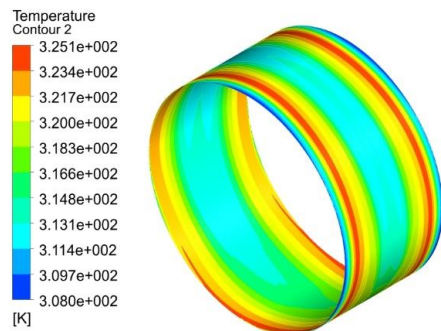
e) Temperature distribution contour for 1000RPM



f) Temperature distribution contour for 2000RPM



g) Temperature distribution contour for 3000RPM



h) Temperature distribution contour for 4000RPM

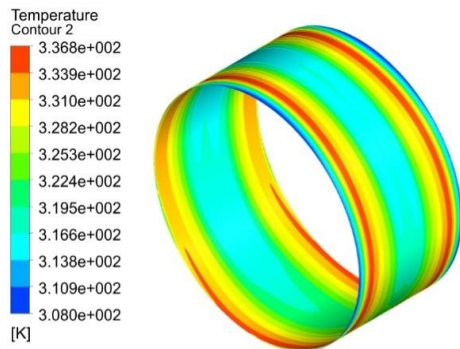


Fig -3: The film pressure and temperature distribution contours for $\epsilon = 0.4$ at various shaft speeds

5.1 Effect of rotational speed:

It is observed that as the speed increases, the value of peak pressure increases. The pressure distribution is wide for lower speeds but becomes narrower with increase in speed. The value of maximum temperature also increases with speed.

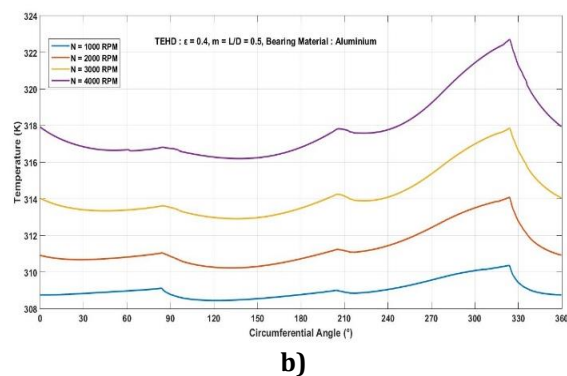
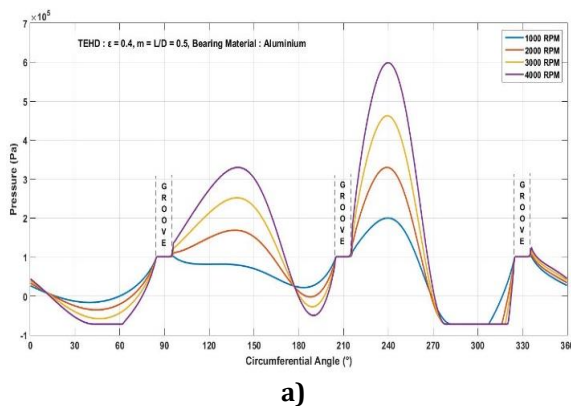


Chart-1: Comparison of circumferential flow field distribution for CFD at various shaft speeds and $\epsilon = 0.4$ for a) pressure and b) temperature

5.2 Effect of eccentricity ratio:

As the eccentricity ratio increases, the peak pressure value also increases. But the peak pressure shifts to lobe three where minimum film thickness lies and the multilobe effect is lost and bearing starts behaving like plain journal

bearing. Maximum values of the temperature also increase with increase in eccentricity ratio.

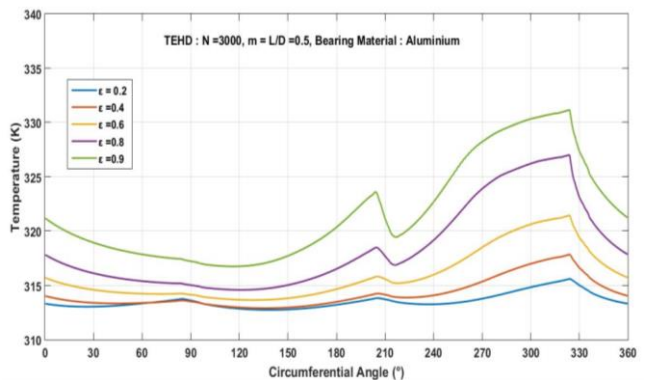
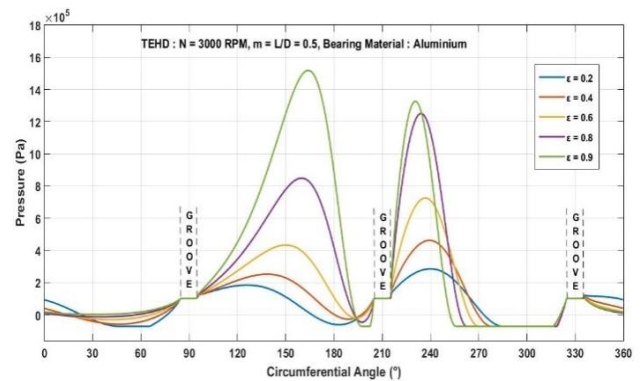


Chart-2: Comparison of circumferential flow field distribution for CFD at various Eccentricity Ratios and $N=3000RPM$ for a) pressure and b) temperature

5.3 Effect of two-way FSI:

It is observed from the figure that, by using two-way FSI model in the system coupling, the deformation of the bearing shell occurs, the peak pressure value decreases. This is due to the fact that, the bearing deformation increases the clearance space therefore allowing more flow of fluid and thus decreasing the peak pressure value. The peak value of pressure again further drops due to thermal deformation effect.

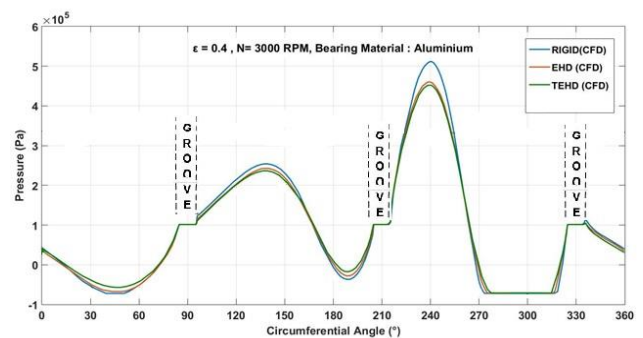


Chart-3: Comparison of circumferential pressure distribution for CFD at shaft speeds $N = 3000RPM$ and $\epsilon=0.4$ for rigid, elastohydrodynamics and thermoelastohydrodynamics

6. CONCLUSIONS

The present work is an application of numerical solution to the three-lobe bearing comprising of CFD and FSI methodology. It is observed that three-lobe bearing gives three pressure contours due to non-circular geometry. In the temperature plots, it is observed that decrease in the slope of profile which is due to three inlet grooves provide 120° apart. The peak pressure increases with an increase in both speed as well as eccentricity ratio, but more sensitive to eccentricity ratio change. Two-way Fluid–structure interaction lowers the values of peak pressure due to bearing deformation due to elastic as well as thermal effect.

REFERENCES

- [1]. R. Sinhasan, M. Malik and M. Chandra, “A comparative study of some three-lobe bearing configurations”, wear, 1981, 72, pp. 277 – 286.
- [2]. S. C. Jain, R. Sinhasan and D. V. Singh, “The performance characteristics of thin compliant shell journal bearings”, Wear, 1982, pp.251 –261.
- [3]. Villar M M , Perez M M, “Elastic analysis of Journal Bearings”, 2004, 7th Biennial ASME Conference on Engg. Systems Design and Analysis-ESDA-2004-58533, Manchester.
- [4]. Banwait S S, “A comparative performance analysis of non-circular two-lobe and three-lobe journal bearings, i.e.(i), i, journal of machine components”, 2006, Vol.86, pp.202-210.
- [5]. David V. Taylor, Gregory j. Kostrzewsky, Lloyd E. Barrett & Ronald D. Flack, “Measured performance of highly preloaded three - lobe journal bearing — part I : Static Characteristics”, Tribology Transactions, 2008, Vol. No.38:3 pp.. 507-516.
- [6]. Dr. Luis San Anders, “Dynamics of rigid rotor – fluid film bearing system”, 2010.
- [7]. Zhi Li, Lihua Yang, Jian Zhou and Lie Yu, “Pressure distribution for multi-lobe bearings using Fourier analysis”, 2014, journal of Engineering Tribology, Vol. No 229(5), pp. 624-635.
- [8]. Athanasios Chasalevris, “Analytical evaluation of the static and dynamic characteristics of three-lobe journal bearings with finite length”, 2014, Journal of tribology, pg.1-80, doi:10.1115/1.
- [9]. D.Y. Dhande, D.W. Pande, “Multiphase flow analysis of hydrodynamic journal bearing using CFD coupled Fluid Structure Interaction considering cavitation”, 2016, Journal of king saud university, pp.1018-3639.